JOURNAL OF GUIDANCE, CONTROL, AND DYNAMICS
Vol. 29, No. 5, September–October 2006

Parametric Model and Optimal Control of Solar Sails with Optical Degradation

Bernd Dachwald*
DLR, German Aerospace Center, 51147 Cologne, Germany
Giovanni Mengali† and Alessandro A. Quarta‡
University of Pisa, 56122 Pisa, Italy
and
Malcolm Macdonald§
University of Glasgow, Glasgow, Scotland G12 8QQ, United Kingdom

Solar-sail mission analysis and design is currently performed assuming constant optical and mechanical properties of the thin metalized polymer films that are projected for solar sails. More realistically, however, these properties are likely to be affected by the damaging effects of the space environment. The standard solar-sail force models can therefore not be used to investigate the consequences of these effects on mission performance. The aim of this paper is to propose a new parametric model for describing the sail film's optical degradation with time. In particular, the sail film's optical coefficients are assumed to depend on its environmental history, that is, the radiation dose. Using the proposed model, the optimal control laws for degrading solar sails are derived using an indirect method and the effects of different degradation behaviors are investigated for an example interplanetary mission.

Nomenclature

A	=	sail area
a	=	absorption coefficient
a_c	=	characteristic acceleration
$\boldsymbol{a}_d$	=	sailcraft disturbing acceleration
$\boldsymbol{a}_{\mathrm{SRP}}$	=	sailcraft propulsive acceleration (SRP = solar radiation pressure)
a_1, a_2, a_3	=	force coefficients
B	=	non-Lambertian coefficient
b_1, b_2, b_3	=	force coefficients
c	=	speed of light in vacuum
d	=	degradation factor
$\boldsymbol{e}_r, \boldsymbol{e}_t, \boldsymbol{e}_h$	=	unit vectors of the orbital reference frame
$\boldsymbol{e}_x, \boldsymbol{e}_y, \boldsymbol{e}_z$	=	unit vectors of the inertial reference frame
$\boldsymbol{F}$	=	force vector
f	=	dimensionless force
$\mathcal{H}$	=	Hamiltonian
$\mathcal{H}'$	=	portion of $\mathcal{H}$ that explicitly depends on the controls
$\mathcal{I}$	=	inertial reference frame
m	=	sailcraft mass
$\boldsymbol{m}$	=	thrust unit vector
$\boldsymbol{n}$	=	sail normal (unit) vector
$\mathcal{O}$	=	orbital reference frame
P	=	solar radiation pressure
$\mathcal{P}$	=	set of optical coefficients
p	=	arbitrary optical coefficient $\in \mathcal{P}$
$\boldsymbol{r}$	=	position vector ($r \triangleq \|\boldsymbol{r}\|$)
r_0	=	1 astronomical unit (AU)
S	=	solar radiation flux
$\mathcal{S}$	=	sail-fixed reference frame
S_{pf}	=	solar particle flux
S_0	=	solar constant
s	=	specular reflection factor
T	=	sail equilibrium temperature
T_Σ	=	reference time
t	=	time
$\boldsymbol{t}$	=	sail tangential (unit) vector
$\mathcal{U}$	=	domain of feasible controls
$\boldsymbol{u}$	=	control vector
$\boldsymbol{v}$	=	velocity vector
W	=	power
$\boldsymbol{x}$	=	state vector
$\boldsymbol{z}$	=	vector that contains the solar distance and the sail attitude
α	=	sail pitch angle
β	=	lightness number
β_σ	=	dimensionless sail loading
δ	=	sail clock angle
ε	=	emission coefficient
θ	=	sail cone angle
λ	=	degradation constant
$\boldsymbol{\lambda}_r$	=	vector adjoint to the position
$\boldsymbol{\lambda}_v$	=	primer vector
$\boldsymbol{\lambda}_\Sigma$	=	costate associated to Σ
μ	=	sun's gravitational parameter
ρ	=	reflection coefficient
Σ	=	solar radiation dose
$\tilde{\Sigma}$	=	dimensionless solar radiation dose
$\hat{\Sigma}$	=	half-life solar radiation dose
σ	=	sail loading
σ_0	=	reference sail loading
$\tilde{\sigma}$	=	Stefan–Boltzmann constant
τ	=	transmission coefficient
ϕ	=	centerline angle
Ψ	=	force function [see Eq. (6)]

Received 29 September 2005; revision received 17 November 2005; accepted for publication 28 November 2005. Copyright © 2006 by the American Institute of Aeronautics and Astronautics, Inc. All rights reserved. Copies of this paper may be made for personal or internal use, on condition that the copier pay the $10.00 per-copy fee to the Copyright Clearance Center, Inc., 222 Rosewood Drive, Danvers, MA 01923; include the code 0731-5090/06 $10.00 in correspondence with the CCC.

*Scientist; currently Project Manager, DLR, German Aerospace Center, Mission Operations Section, Oberpfaffenhofen, 82230 Wessling, Germany; bernd.dachwald@dlr.de. Member AIAA.

†Associate Professor, Department of Aerospace Engineering; g.mengali@ing.unipi.it.

‡Research Assistant, Department of Aerospace Engineering; a.quarta@ing.unipi.it.

§Research Assistant; currently AOCS Engineer, SciSys, Software Engineering Group, Bristol, England BS4 5SS, United Kingdom; malcolm.macdonald@scisys.co.uk.

Subscripts

b	=	back reflection
b	=	sail backside
d	=	diffuse reflection
f	=	final
f	=	sail front side
max	=	maximum
r	=	orbit radial
SRP	=	solar radiation pressure
s	=	specular reflection
t	=	orbit transversal
λ	=	primer vector
0	=	initial; reference; at 1 astronomical unit
∞	=	end of life
$\parallel$	=	sail tangential
$\perp$	=	sail normal

Superscripts

$\cdot$	=	time derivative
$*$	=	corresponding to the maximum orbit transversal force

Introduction

SOLAR-SAIL technology has been identified as enabling for many recent space mission concepts because of its capability of reducing the mission costs and increasing the payload mass fraction. Moreover, the continuous advances in material technology can enable near-term solar-sail missions that would be prohibitive for other types of primary propulsion.[1] A realistic mission analysis, however, is a demanding task because solar-sail performance is significantly affected by both the sail geometry[2] and the optical properties of the sail film.[3]

An imperfectly reflecting sail model, described in Refs. 4–6, is widely used for solar-sail mission analysis, even if most of the currently available results have been obtained using an even simpler model with ideal reflection. Assuming imperfectly reflecting sail characteristics, Rios-Reyes and Scheeres have recently proposed a generalized sail model for nonflat solar sails, which allows one to take into account also the local variation effects of the optical sail properties.[7] Nevertheless, all of the preceding models are still quite unsatisfactory because the optical and mechanical properties of the thin metalized solar-sail polymer films are assumed to be constant.

The objective of this paper is to propose a more realistic mathematical model that includes optical solar-sail degradation and to derive the corresponding optimal control laws for degrading solar sails. The starting point of our discussion is the ascertainment that the optical and mechanical properties of solar-sail films are degraded by the harsh space environment. Optical solar-sail degradation (OSSD) should be considered for a thorough solar-sail mission analysis because this effect not only decreases the magnitude of the solar radiation pressure (SRP) force acting on the sail, but also the sail control authority, as it reduces the magnitude of the SRP force component perpendicular to the sun-sail direction. Mechanical solar-sail degradation (MSSD) should also be considered in the solar-sail design process because it decreases the tensile strength of the sail film and thus can affect the sail performance. MSSD, however, is not considered within this paper because its effects depend on the actual mechanical strain in the sail film and, therefore, on he actual solar-sail design.

Although significant ground and space testing has been performed to measure the optical degradation of metalized polymer films as second surface mirrors (metalized on the backside), to our knowledge no systematic testing has been reported so far to measure the optical degradation of candidate solar-sail films (metalized on the front side) either on ground or in space. As such, the optical degradation behavior of solar sails and therefore the degradation behavior of the sail's propulsive capability in the real space environment is still, to a great extent, indefinite. Nevertheless, solar-sail mission designers require an OSSD model to estimate the potential effects of OSSD on their preliminary studies. Therefore, the authors of this paper established in November 2004 a working group (see Acknowledgments) to take a step forward towards the definition of a realistic optical solar-sail model, by elaborating a parametric model for OSSD. This model describes the variation of the sail film's optical coefficients with time, through a dependence on the sail film's environmental history, that is, the radiation dose. The primary intention of this model is not that of describing the exact behavior of specific film-coating combinations in the real space environment, but rather that of providing a flexible parametric framework for representing the general optical degradation behavior of solar sails. Of course the proposed model is susceptible to further refinements, especially when the results obtained from both ground and in-space tests would become available. Until then, our model can be used to investigate the effects of different potential degradation behaviors on various mission aspects, for example, trajectory optimization and attitude control, by simply varying the OSSD model parameters.

The paper is organized as follows. First, the SRP force model for imperfectly reflecting solar sails is briefly reviewed. Starting from that, a new parametric OSSD model describing the variation of the sail film's optical coefficients with time is introduced through a dependence of the coefficients on the radiation dose. This model is then used to derive the optimal control law for degrading solar sails and to estimate the effects of this OSSD model on the minimum trip time and the optimal steering law for an example Mars rendezvous mission.

Solar-Radiation-Pressure Force Model

The description of the SRP force exerted on a solar-sail is better understood with the introduction of two unit vectors. The first one is the sail normal vector $\boldsymbol{n}$, which is perpendicular to the sail surface and always directed away from the sun. The second one is the thrust unit vector $\boldsymbol{m}$, which points along the direction of the SRP force. Let $\mathcal{O}^3 = \{\boldsymbol{e}_r, \boldsymbol{e}_t, \boldsymbol{e}_h\}$ be an orthogonal right-handed polar coordinate frame, where $\boldsymbol{e}_r$ points along the sun-spacecraft line, $\boldsymbol{e}_h$ is normal to the orbit plane (pointing along the spacecraft's orbital angular momentum vector), and $\boldsymbol{e}_t$ completes the right-handed coordinate system. In $\mathcal{O}^3$, the direction of the sail normal vector $\boldsymbol{n}$, which describes the sail attitude, is expressed through the pitch angle α and the clock angle δ, while the direction of the thrust unit vector $\boldsymbol{m}$ is described by the cone angle θ and the clock angle δ (see Fig. 1).

At a distance r from the sun, the SRP is

$$P = (S_0/c)(r_0/r)^2 = P_0 \cdot (r_0/r)^2 = 4.563\,\mu\mathrm{N/m^2} \cdot (r_0/r)^2 \quad (1)$$

where $S_0 = 1368$ W/m^2 is the solar constant.

Different levels of simplification for the optical characteristics of a solar sail result in different models for the magnitude and direction of the SRP force. The most simple model assumes an ideally reflecting sail surface. It will here be denoted as model IR (ideal reflection). The SRP force exerted on an ideal sail

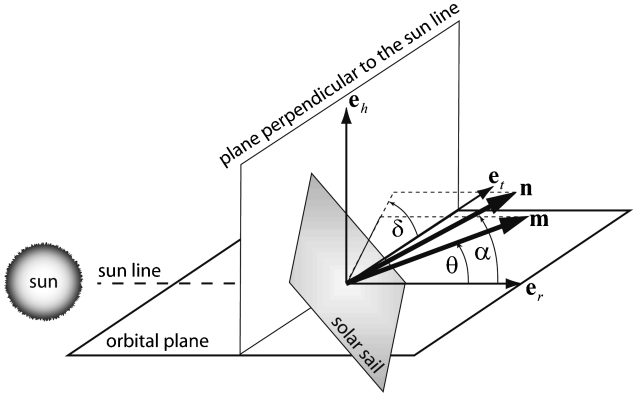

Fig. 1 Definition of the sail normal vector and the thrust unit vector.

of area A is[5]

$$\boldsymbol{F}_{\mathrm{SRP}} = 2PA\cos^2\alpha\boldsymbol{n} \tag{2}$$

For a thorough mission analysis and design, however, a more sophisticated SRP force model than IR must be employed, which takes into account the optical coefficients of the real sail film. This model will be referred to as model NPR (nonperfect reflection). It was proposed in the 1970s for solar-sail trajectory optimization by Sauer[8] and further studied by Forward,[4] but found little application until recently.[3,9–12]

Optical Solar-Sail Coefficients

In model NPR the optical characteristics of the sail film are parameterized through the absorption coefficient a, the reflection coefficient ρ, the transmission coefficient τ, and the emission coefficient ε, with the constraint $a+\rho+\tau=1$. Assuming $\tau=0$ for the reflecting side of the solar sail, the absorption coefficient is $a=1-\rho$. Because not all of the photons are reflected specularly, the reflection coefficient can be further divided into a specular reflection coefficient ρ_s, a diffuse reflection coefficient ρ_d, and a back-reflection coefficient ρ_b, with the constraint $\rho_s+\rho_d+\rho_b=\rho$. Assuming $\rho_b=0$, the latter constraint can equivalently be expressed by introducing a specular reflection factor s, such that $\rho_s=s\rho$ and $\rho_d=(1-s)\rho$. The emission coefficient ε describes the power W that is emitted from a surface of area A at absolute temperature T, $W=A\varepsilon\tilde{\sigma}T^4$, where $\tilde{\sigma}=5.67\cdot10^{-8}$ $\mathrm{Wm^{-2}K^{-4}}$ is the Stefan–Boltzmann constant. The emission coefficients of the sail's front and backside are ε_f and ε_b, respectively. The angular distribution of the emitted and diffusely reflected photons is described by the non-Lambertian coefficients of the sail's front and backside, B_f and B_b, respectively. As a result, model NPR parameterizes the optical characteristics of the sail film by the following set of six optical coefficients: $\mathcal{P}=\{\rho, s, \varepsilon_f, \varepsilon_b, B_f, B_b\}$. According to Wright,[5] the optical coefficients for a sail with a highly reflective aluminum-coated front side and a highly emissive chromium-coated backside are $\mathcal{P}_{\mathrm{Al|Cr}}=\{\rho=0.88, s=0.94, \varepsilon_f=0.05, \varepsilon_b=0.55, B_f=0.79, B_b=0.55\}$.

Solar Radiation Pressure Force

Using the optical sail coefficients just defined, the SRP force exerted on the solar sail can be decomposed in a sail-fixed two-dimensional coordinate frame $S=\{\boldsymbol{n},\boldsymbol{t}\}$ (because of symmetry, the third dimension is not relevant here) through a normal component $F_\perp$ along $\boldsymbol{n}$ and a tangential component $F_{||}$ along $\boldsymbol{t}$ (see Fig. 2), where

$$F_\perp = \boldsymbol{F}_{\mathrm{SRP}}\cdot\boldsymbol{n} = 2PA\cos\alpha\,(a_1\cos\alpha + a_2) \tag{3a}$$

$$F_{||} = \boldsymbol{F}_{\mathrm{SRP}}\cdot\boldsymbol{t} = -2PA\cos\alpha\, a_3\sin\alpha \tag{3b}$$

with

$$a_1 \triangleq \frac{1}{2}(1+s\rho) \tag{4a}$$

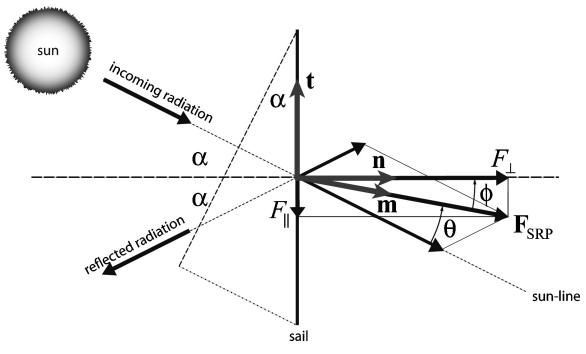

Fig. 2 SRP force on an imperfectly reflecting sail.

$$a_2 \triangleq \frac{1}{2}\left[B_f(1-s)\rho + (1-\rho)\frac{\varepsilon_f B_f - \varepsilon_b B_b}{\varepsilon_f+\varepsilon_b}\right] \tag{4b}$$

$$a_3 \triangleq \frac{1}{2}(1-s\rho) \tag{4c}$$

The total SRP force vector can then be written as

$$\boldsymbol{F}_{\mathrm{SRP}} = 2PA\cos\alpha\,\Psi\,\boldsymbol{m} \tag{5}$$

with

$$\Psi \triangleq \left[(a_1\cos\alpha + a_2)^2 + (a_3\sin\alpha)^2\right]^{\frac{1}{2}} \tag{6}$$

where Ψ depends only on the pitch angle α and the optical coefficients $\mathcal{P}$ of the sail film. Note the symmetry in Eqs. (2) and (5). Recall that the angle between $\boldsymbol{m}$ and $\boldsymbol{e}_r$ is the cone angle θ, whereas the angle between $\boldsymbol{m}$ and $\boldsymbol{n}$ is referred to as centerline angle ϕ. It can be calculated via

$$\phi = \arctan\left(\frac{a_3\sin\alpha}{a_1\cos\alpha + a_2}\right) \tag{7}$$

From Eq. (7), the cone angle is then obtained as $\theta=\alpha-\phi$.

The SRP force can also be written in terms of components along the unit vectors of a two-dimensional orbit frame $\mathcal{O}=\{\boldsymbol{e}_r,\boldsymbol{e}_t\}$, a decomposition that will be used in the next section to investigate the relative importance of the various optical coefficients $p\in\mathcal{P}$ for OSSD modeling. The $\mathcal{O}$-frame components of $\boldsymbol{F}_{\mathrm{SRP}}$ are obtained from the $\mathcal{S}$-frame components via

$$\begin{pmatrix}F_r\\F_t\end{pmatrix} = \begin{bmatrix}\cos\alpha & -\sin\alpha\\ \sin\alpha & \cos\alpha\end{bmatrix}\begin{pmatrix}F_\perp\\F_{||}\end{pmatrix} \tag{8}$$

so that

$$F_r = \boldsymbol{F}_{\mathrm{SRP}}\cdot\boldsymbol{e}_r = 2PA\cos\alpha\left(a_1\cos^2\alpha + a_2\cos\alpha + a_3\sin^2\alpha\right) \tag{9a}$$

$$F_t = \boldsymbol{F}_{\mathrm{SRP}}\cdot\boldsymbol{e}_t = 2PA\cos\alpha\sin\alpha(a_1\cos\alpha + a_2 - a_3\cos\alpha) \tag{9b}$$

Finally, the SRP force can be written also in terms of components along $\boldsymbol{e}_r$ and $\boldsymbol{n}$, a decomposition that is useful for the derivation of the optimal control law, as shown later. The result is[12]

$$\boldsymbol{F}_{\mathrm{SRP}} = 2PA\cos\alpha[b_1\boldsymbol{e}_r + (b_2\cos\alpha + b_3)\boldsymbol{n}] \tag{10}$$

where the coefficients b_1, b_2, and b_3 are defined as

$$b_1 \triangleq \frac{1}{2}(1-s\rho) \tag{11a}$$

$$b_2 \triangleq s\rho \tag{11b}$$

$$b_3 \triangleq \frac{1}{2}\left[B_f(1-s)\rho + (1-\rho)\frac{\varepsilon_f B_f - \varepsilon_b B_b}{\varepsilon_f+\varepsilon_b}\right] \tag{11c}$$

Optical SRP Force Sensitivity

To obtain dimensionless expressions, the components of $\boldsymbol{F}_{\mathrm{SRP}}$ in the $\mathcal{O}^2$ frame can be divided by the SRP force acting on a blackbody with an area A perpendicular to the incoming radiation, that is, $f_r \triangleq F_r/PA$ and $f_t \triangleq F_t/PA$. Then, the sensitivity of f_r and f_t with respect to the various optical coefficients p can be described as

$$\frac{\partial f_r}{\partial p} = \cos\alpha(P_{p1}\cos\alpha + P_{p2}\cos 2\alpha) \tag{12a}$$

$$\frac{\partial f_t}{\partial p} = \cos\alpha\sin\alpha(P_{p1} + 2P_{p2}\cos\alpha) \tag{12b}$$

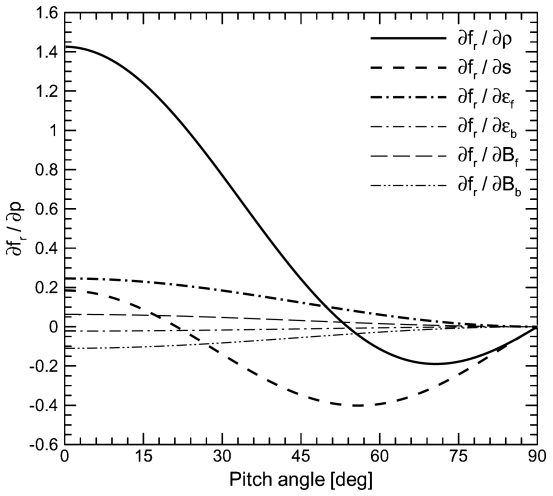

a) $\partial f_r/\partial p$

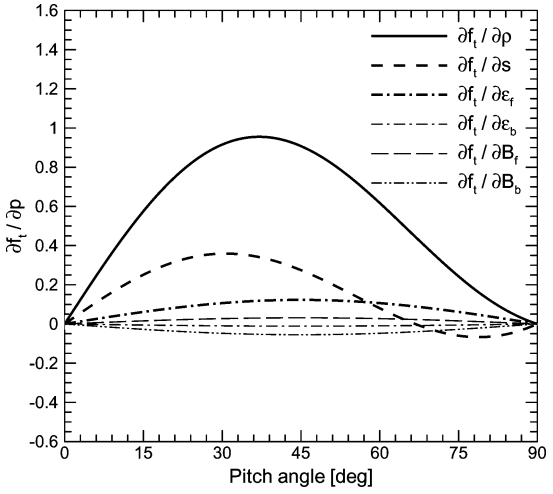

b) $\partial f_t/\partial p$

Fig. 3 Sensitivity of the SRP force components with respect to the optical coefficients.

Using the optical parameters of an Al|Cr-coated sail, one gets $P_{\rho 1} = 0.4857\bar{3}$, $P_{\rho 2} = 0.94$, $P_{s1} = -0.6952$, $P_{s2} = 0.88$, $P_{\varepsilon_f 1} = 0.245\bar{6}$, $P_{\varepsilon_b 1} = -0.022\bar{3}$, $P_{B_f 1} = 0.0628$, $P_{B_b 1} = -0.11$, and $P_{\varepsilon_f 2} = P_{\varepsilon_b 2} = P_{B_f 2} = P_{B_b 2} = 0$. Figure 3 shows how the SRP force components f_t and f_r vary with α. Note that the sensitivity of f_t and f_r is largest with respect to ρ, s, and ε_f. The sensitivity with respect to the other optical coefficients is only minor and can be neglected for a first OSSD analysis.

Sail Performance Parameters

The performance of a solar sail is usually quantified through the values taken by the characteristic acceleration and the lightness number. The characteristic acceleration a_c is defined as the SRP acceleration acting on a solar sail that is oriented perpendicular to the sun line ($\boldsymbol{n} \equiv \boldsymbol{e}_r$) at r_0 (1 AU). For model IR the result is

$$a_c = 2P_0 A/m \tag{13}$$

and for model NPR

$$a_c = (2P_0 A/m)(a_1 + a_2) \tag{14}$$

The lightness number β, instead, is defined as the ratio of the SRP acceleration acting on a solar sail that is oriented perpendicular to the sun line ($\boldsymbol{n} \equiv \boldsymbol{e}_r$), and the gravitational acceleration of the sun μ/r^2:

$$\beta = \frac{a_c (r_0/r)^2}{\mu/r^2} = \frac{a_c}{\mu/r_0^2} \tag{15}$$

where $\mu/r_0^2 \doteq 5.930\,\text{mm/s}^2$ is the sun's gravitational acceleration at Earth distance. Another possible way to define a lightness number is by thinking of it as a dimensionless sail loading, that is, $\beta_\sigma \triangleq \sigma_0/\sigma$, where $\sigma \triangleq m/A$ is the sail loading and $\sigma_0 \triangleq 2P_0/(\mu/r_0^2) = 1.539\ \text{g/m}^2$ is a reference sail loading parameter. As a result, β_σ plays the role of a technological parameter in that it establishes the limits of the current (or future) sail technology. With this definition one gets

$$a_c = \beta_\sigma (a_1 + a_2)\left(\mu/r_0^2\right) \tag{16}$$

or

$$\beta_\sigma = \left[\frac{a_c}{\left(\mu/r_0^2\right)}\right]\left[\frac{1}{(a_1 + a_2)}\right] = \frac{\beta}{(a_1 + a_2)} \tag{17}$$

Equation (17) shows that, in general, $\beta_\sigma \neq \beta$. Note, however, that for model IR $a_1 + a_2 = 1$, and $\beta_\sigma \equiv \beta$. To avoid ambiguity, we will use β as the lightness number for the remainder of this paper.

Imperfectly Reflecting Solar Sail with Degradation

Data Available from Ground Testing

Although significant ground and space testing has been performed to measure the optical degradation of metalized polymer films as second surface mirrors (metalized on the backside), to our knowledge, no systematic testing to measure the optical degradation of candidate solar-sail films (metalized on the front side) has been reported so far. Lura et al.[13] pointed out the considerable OSSD effects caused by a combined irradiation with vacuum ultraviolet (VUV) radiation, electrons, and protons, whereas Edwards et al.[14] emphasized that a change of the solar absorption and emission coefficients cannot be measured after irradiation with electrons alone. Because a corresponding in-space testing campaign has not yet been done, the optical degradation behavior of solar sails, and therefore the degradation behavior of the sail propulsive capability in the real space environment, is, to a great extent, indefinite. Nevertheless, solar-sail mission designers require an OSSD model to estimate the potential effects of OSSD on their missions. This is the subject of the next section.

Parametric Degradation Model

To establish a first OSSD model, the following simplifications are assumed:

1) The only source of degradation is the solar photons and particles. This simplification is reasonable at least in the inner solar system and far from the planets, where the cosmic radiation, the radiation from the planetary radiation belts, and the reactions with particles of the planetary atmospheres can be neglected.

2) The solar photon and particle fluxes do not depend on time (average sun without solar events).

3) The optical coefficients do not depend on the sail temperature.

4) The optical coefficients do not depend on the light incidence angle.

5) No self-healing effects occur in the sail film.

Let p be an arbitrary optical coefficient taken from $\mathcal{P}$. Using an OSSD model, p becomes a time-dependent coefficient, $p = p(t)$. With the preceding simplifications, $p(t)$ is a function of the solar radiation dose [SRD, dimension (J/m^2)] accepted by the solar sail within the time interval $t - t_0$:

$$\tilde{\Sigma}(t) \triangleq \int_{t_0}^{t} S \cos\alpha \, \mathrm{d}t' = S_0 r_0^2 \int_{t_0}^{t} \frac{\cos\alpha}{r^2} \, \mathrm{d}t' \tag{18}$$

The symbol $\tilde{\Sigma}$ is used for the SRD, this way preserving Σ for the dimensionless SRD. The SRD per year on a surface that is perpendicular to the sun at 1 AU is $\tilde{\Sigma}_0 = S_0 \cdot 1\ \text{yr} = 1368\ \text{W/m}^2 \cdot 1\ \text{yr} = 15.768\ \text{TJ/m}^2$. Using $\tilde{\Sigma}_0$ as a reference value, the SRD can be defined in a dimensionless form as

$$\Sigma(t) \triangleq \frac{\tilde{\Sigma}(t)}{\tilde{\Sigma}_0} = \left(r_0^2 \int_{t_0}^{t} \frac{\cos\alpha}{r^2} \, \mathrm{d}t'\right) \Big/ 1\ \text{yr} \tag{19}$$

Because the solar particle flux S_{pf} also varies as $\cos\alpha/r^2$, its dose within the time interval $t - t_0$ can be written as $\Sigma_{\mathrm{pf}}(t) = \gamma_{\mathrm{pf}}\Sigma(t)$, such that

$$p(t) = p[\Sigma(t) + \Sigma_{\mathrm{pf}}(t)] = p[(1+\gamma_{\mathrm{pf}})\Sigma(t)] = p[\Sigma(t)] \quad (20)$$

As a result, the degradation effects of the solar particles do not have to be considered separately. $\Sigma(t)$ depends on the solar distance history and the attitude history $z[t] \triangleq (r, \alpha)[t]$ of the solar sail, $\Sigma(t) = \Sigma(z[t])$. Note that Eq. (19) can be rearranged in differential form as

$$\dot{\Sigma}(t) = \left(r_0^2 \big/ T_\Sigma\right)(\cos\alpha/r^2) \quad \text{with} \quad \Sigma(t_0) = 0 \quad (21)$$

where $T_\Sigma \triangleq 1\mathrm{yr}$. We assume that $p(t)$ varies exponentially between $p(t_0) = p_0$ and $\lim_{t\to\infty} p(t) = p_\infty$, that is,

$$p(t) = p_\infty + (p_0 - p_\infty)\cdot e^{-\lambda\Sigma(t)} \quad (22)$$

The degradation constant λ is related to the half-life solar radiation dose $\hat{\Sigma}$ [that is, $\Sigma = \hat{\Sigma}$ implies $p = (p_0 + p_\infty)/2$] via

$$\lambda = \ell_n 2/\hat{\Sigma} \quad (23)$$

Note that this model has 12 free parameters in addition to the six p_0, six p_∞, and six half-life SRDs $\hat{\Sigma}_p$. Because 12 parameters are hardly manageable in a parametric OSSD analysis, the number of free parameters should be reduced. To this end, a degradation factor d and a single-half life SRD for all p, $\hat{\Sigma}_p = \hat{\Sigma}\ \forall p \in \mathcal{P}$, are introduced. Because when time increases, the reflectivity of the sail decreases, the sail becomes more matt, and the emissivity increases, and we assume that

$$\rho_\infty = \rho_0/(1+d) \quad (24a)$$

$$s_\infty = s_0/(1+d) \quad (24b)$$

$$\varepsilon_{f_\infty} = (1+d)\varepsilon_{f_0} \quad (24c)$$

$$\varepsilon_{b_\infty} = \varepsilon_{b_0} \quad (24d)$$

$$B_{f_\infty} = B_{f_0} \quad (24e)$$

$$B_{b_\infty} = B_{b_0} \quad (24f)$$

(Recalling from Fig. 3 that ε_b, B_f, and B_b are of minor importance for OSSD, it is justified to assume them to be constant.) The degradation of the optical parameters can be written in dimensionless form as

$$\frac{p(t)}{p_0} = \begin{cases} (1 + d\mathrm{e}^{-\lambda\Sigma(t)})/(1+d) & \text{for} \quad p \in \{\rho, s\} \\ 1 + d\left(1 - \mathrm{e}^{-\lambda\Sigma(t)}\right) & \text{for} \quad p = \varepsilon_f \\ 1 & \text{for} \quad p \in \{\varepsilon_b, B_f, B_b\} \end{cases} \quad (25)$$

Figure 4a shows the variation of those coefficients with Σ for different values of the degradation factor d. With such a model, the a/ε_f ratio ranges between

$$a_0/\varepsilon_{f_0} = (1-\rho_0)/\varepsilon_{f_0} = 2.4$$

and

$$\frac{a_\infty}{\varepsilon_{f_\infty}} = \frac{1+d-\rho_0}{(1+d)^2\varepsilon_{f_0}}$$

whose value is 3.1 for a 5% degradation limit, 3.6 for a 10% degradation limit, and 4.4 for a 20% degradation limit. (To preserve a simple terminology, we will use the term "a 100 d% degradation limit" synonymous with "a degradation factor of d.") Figure 4b shows how the maximum sail temperature[6] $T_{\max} = [S_0/\tilde{\sigma}\cdot a/(\varepsilon_f + \varepsilon_b)\cdot(r_0/r)^2]^{1/4}$ (for $\alpha = 0$) varies with Σ for different solar distances in the range

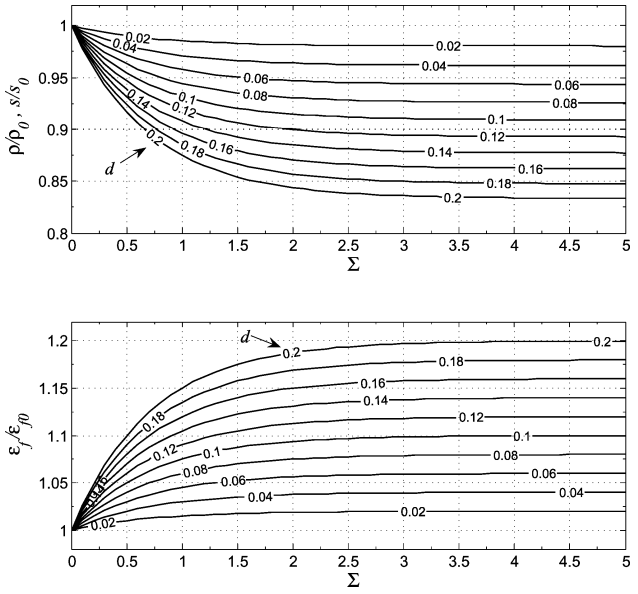

a) Variation of ρ/ρ_0, s/s_0, and $\varepsilon_f/\varepsilon_{f_0}$ with Σ

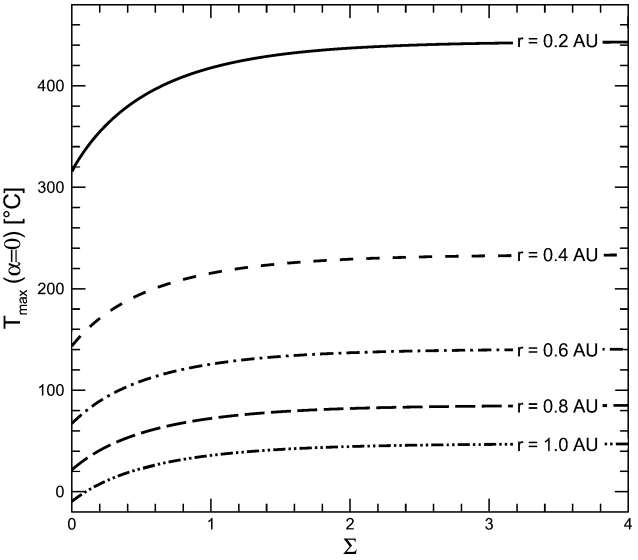

b) Variation of $T_{\max}$ with Σ for different solar distances ($d = 0.2$)

Fig. 4 OSSD of the optical parameters and its effect on the sail temperature.

$0.2\ \mathrm{AU} \le r \le 1\ \mathrm{AU}$. Figure 5a shows the evolution of the $\boldsymbol{F}_{\mathrm{SRP}}$ bubble (the bubble on which surface the tip of the $\boldsymbol{F}_{\mathrm{SRP}}$ vector is constrained to lie) with increasing SRD, and Fig. 5b shows the evolution of the difference between the pitch and cone angle with increasing SRD. Let $F_t^* = \max_\alpha F_t$ denote the maximum SRP force component along $\boldsymbol{e}_t$ (the direction along which the orbital energy is most effectively changed), α^* the pitch angle that corresponds to F_t^*, and θ^* the associated cone angle. Figure 5c shows their variation with SRD.

Note that the OSSD model described here can be directly applied to the generalized sail model (GSM) detailed in Ref. 7. The GSM is able to model nonflat sails and more complex sail geometries, using the flat-plate model given in Eqs. (3) and (4) to define differential sail properties. Because the GSM uses the same optical parameters as those of Eq. (4), the effect of optical sail degradation can be modeled accordingly. As such, the OSSD model can be immediately translated into a more realistic GSM.

Equations of Motion

Besides the gravitational forces of all celestial bodies and the SRP force, many disturbing forces, caused, for example, by the solar wind, the finiteness of the solar disk, the reflected light from close

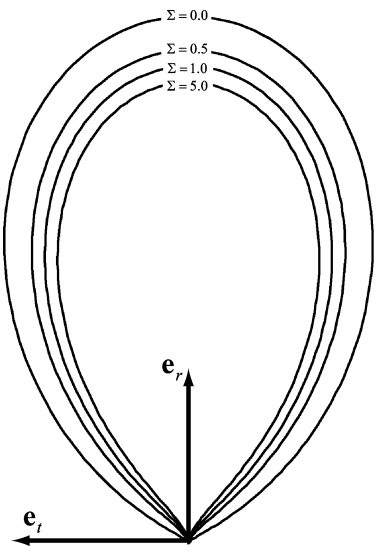

a) Variation of the F_{SRP}-bubble with Σ

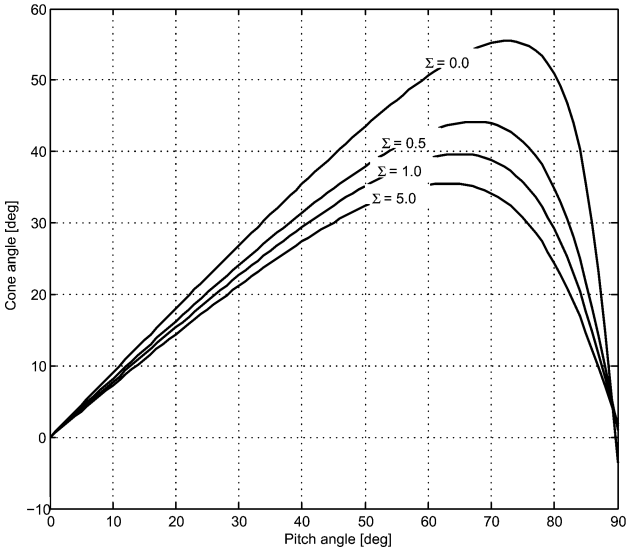

b) Variation of θ with α for different values of Σ

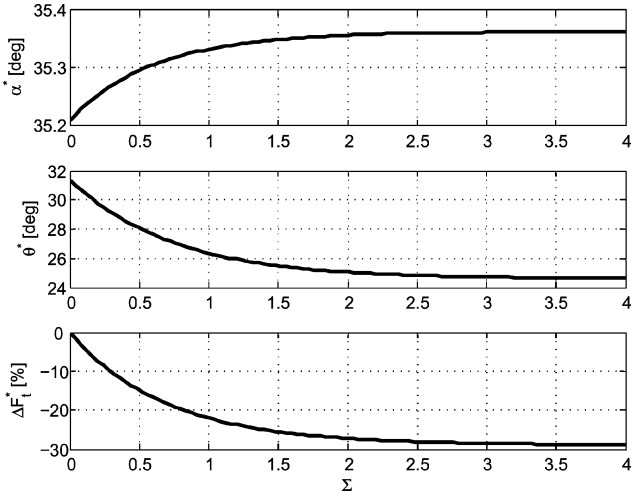

c) Variation of α^*, θ^*, and ΔF_t^* with Σ

Fig. 5 OSSD effects on sail steering ($d = 0.2$).

celestial bodies, and the aberration of solar radiation (Poynting–Robertson effect), influence the motion of solar sails in space. Furthermore, a real solar sail bends and wrinkles, depending on the actual sailcraft design. In principle, all of these effects should be taken into account for a high-precision trajectory determination.

However, for purposes of mission feasibility analysis and to isolate the effects of OSSD from the other effects that influence the motion of real solar sails in space, the following simplifications are made:

1) The solar sail is a flat plate.

2) The solar sail is moving under the sole influence of solar gravitation and radiation.

3) The sun is a point mass and a point light source.

4) The solar-sail attitude is changed instantaneously.

Let $\mathcal{I} = \{\boldsymbol{e}_x, \boldsymbol{e}_y, \boldsymbol{e}_z\}$ be an inertial right-handed Cartesian coordinate frame. The equations of motion for a solar sail in the $\mathcal{I}$ frame are

$$\dot{\boldsymbol{r}} = \boldsymbol{v} \tag{26a}$$

$$\dot{\boldsymbol{v}} = -(\mu/r^3)\boldsymbol{r} + \boldsymbol{a} \tag{26b}$$

where $\boldsymbol{r} = (r_x, r_y, r_z)$ is the sailcraft position and $\boldsymbol{v} = (\dot{r}_x, \dot{r}_y, \dot{r}_z) = (v_x, v_y, v_z)$ is the sailcraft velocity, $r = |\boldsymbol{r}|$, μ is the sun's gravitational parameter, and $\boldsymbol{a} = \boldsymbol{a}_{\mathrm{SRP}} + \boldsymbol{a}_d$ is the acceleration acting on the sailcraft ($\boldsymbol{a}_{\mathrm{SRP}}$ being the SRP acceleration and $\boldsymbol{a}_d$ being the disturbing acceleration, which is neglected within this paper). Combining Eqs. (10) and (15), the SRP acceleration is given by

$$\boldsymbol{a}_{\mathrm{SRP}} = \left[\frac{\beta}{(b_1 + b_2 + b_3)}\right]\left(\frac{\mu}{r^2}\right)\cos\alpha[b_1\boldsymbol{e}_r + (b_2\cos\alpha + b_3)\boldsymbol{n}] \tag{27}$$

Although it is often convenient to describe the translational motion of spacecraft in terms of $\mathcal{I}$-frame coordinates, the spacecraft control problem is better analyzed in the reference frame $\mathcal{O}^3 = \{\boldsymbol{e}_r, \boldsymbol{e}_t, \boldsymbol{e}_h\}$. The components of $\boldsymbol{n}$ in the $\mathcal{O}^3$ frame are

$$\boldsymbol{n} = \cos\alpha\boldsymbol{e}_r + \sin\alpha\cos\delta\,\boldsymbol{e}_t + \sin\alpha\sin\delta\,\boldsymbol{e}_h \tag{28}$$

Clearly, α and δ comprise the solar-sail control vector $\boldsymbol{u}$.

Optimal Control Law

The problem is to find the optimal control law $\boldsymbol{u}(t)$ (where $t \in [t_0 = 0, t_f]$), which minimizes the time t_f necessary to transfer the spacecraft from an initial state $\boldsymbol{x}_0 = (\boldsymbol{r}_0, \boldsymbol{v}_0)$ to a final state $\boldsymbol{x}_f = (\boldsymbol{r}_f, \boldsymbol{v}_f)$ by maximizing the performance index $J = -t_f$. From Eq. (26), the Hamiltonian of the system is

$$\mathcal{H} = \boldsymbol{\lambda}_r \cdot \boldsymbol{v} - (\mu/r^3)\boldsymbol{\lambda}_v \cdot \boldsymbol{r} + \boldsymbol{\lambda}_v \cdot \boldsymbol{a} + \lambda_\Sigma\left(r_0^2/r^2 T_\Sigma\right)\boldsymbol{e}_r \cdot \boldsymbol{n} \tag{29}$$

where $\boldsymbol{\lambda}_r$ and $\boldsymbol{\lambda}_v$ are the vectors adjoint to the position and the velocity, respectively, and λ_Σ is the costate associated to Σ. The primer vector[15] $\boldsymbol{\lambda}_v$ can be conveniently expressed in the $\mathcal{O}^3$ frame. Paralleling what has been done for $\boldsymbol{n}$, we define the orientation of

$\boldsymbol{\lambda}_v$ through the angles $\alpha_\lambda \in [0, \pi/2]$ and $\delta_\lambda \in [-\pi, \pi]$ to get

$$\boldsymbol{\lambda}_v = \lambda_v(\cos\alpha_\lambda\, \boldsymbol{e}_r + \sin\alpha_\lambda \cos\delta_\lambda\, \boldsymbol{e}_t + \sin\alpha_\lambda \sin\delta_\lambda\, \boldsymbol{e}_h) \tag{30}$$

where $\lambda_v = |\boldsymbol{\lambda}_v|$. The time derivatives of the adjoint variables are provided by the Euler–Lagrange equations:

$$\dot{\boldsymbol{\lambda}}_r = -\frac{\partial \mathcal{H}}{\partial \boldsymbol{r}}, \qquad \dot{\boldsymbol{\lambda}}_v = -\frac{\partial \mathcal{H}}{\partial \boldsymbol{v}}, \qquad \dot{\lambda}_\Sigma = -\frac{\partial \mathcal{H}}{\partial \Sigma} \tag{31}$$

The explicit form of the partial derivatives is not shown here because of its complexity. Equation (31) provides seven scalar differential equations that must be solved along with the equations of motion, (26) and (21). From Pontryagin's maximum principle, the optimal control law $\boldsymbol{u}(t)$, to be selected in the domain of feasible controls $\mathcal{U}$, is such that at any time the Hamiltonian is an absolute maximum. This amounts to maximizing the function $\mathcal{H}'$, which coincides with that portion of the Hamiltonian $\mathcal{H}$ that explicitly depends on the control vector, that is,

$$\boldsymbol{u} = \arg\max_{u\in\mathcal{U}} \mathcal{H} \equiv \arg\max_{u\in\mathcal{U}} \mathcal{H}' \tag{32}$$

with

$$\mathcal{H}' \triangleq \boldsymbol{\lambda}_v \cdot \boldsymbol{a} + \lambda_\Sigma\left(r_0^2/r^2 T_\Sigma\right)\boldsymbol{e}_r \cdot \boldsymbol{n} \tag{33}$$

Substituting Eqs. (10), (28), and (30) into Eq. (32) and using the necessary condition $\partial\mathcal{H}'/\partial\delta = 0$, one has

$$\tan\delta = \tan\delta_\lambda \tag{34}$$

Equation (34) states that the unit vectors $\boldsymbol{e}_r$, $\boldsymbol{n}$, and $\boldsymbol{e}_{\lambda_v} \triangleq \boldsymbol{\lambda}_v/\lambda_v$ are coplanar. This generalizes a similar conclusion obtained for model NPR without degradation.[12] This result is justified by the fact that $\mathcal{H}'$ depends on the OSSD model through the term $\lambda_\Sigma r_0^2/(r^2 T_\Sigma)\,\boldsymbol{e}_r \cdot \boldsymbol{n}$, which, in turn, is a function of α but not of δ.

As far as the optimal steering law for α is concerned, in contrast to the ideal and optical force model cases,[12,16] an explicit or semi-analytic solution is hardly retrievable. In fact, invoking the necessary condition $\partial\mathcal{H}'/\partial\alpha = 0$, the following equation is obtained for α:

$$b_1[\sin(\alpha+\alpha_\lambda) + \sin(\alpha-\alpha_\lambda)] + (b_2/2)[2\sin(\alpha-\alpha_\lambda) + 3\sin(3\alpha - \alpha_\lambda) + \sin(\alpha+\alpha_\lambda)] + 2b_3\sin(2\alpha-\alpha_\lambda) + b_\Sigma \sin\alpha = 0 \tag{35}$$

where

$$b_\Sigma \triangleq \frac{2r_0^2\lambda_\Sigma}{\beta\mu T_\Sigma \lambda_v}(b_1 + b_2 + b_3) \tag{36}$$

The dimensionless variable b_Σ models the optical degradation of the solar sail. In the ideal case without degradation ($\lambda_\Sigma \equiv 0 \Rightarrow b_\Sigma \equiv 0$), Eq. (35) provides the optimal control law for the optical force model. The corresponding solution is given in Ref. 12. However, when the degradation is taken into account ($\lambda_\Sigma \neq 0$), the situation is more complex. At a generic time instant t and for a given pair (β, d), one can calculate the values taken by b_Σ, Σ, b_1, b_2, and b_3 (which, in turn, depend on Σ, λ, and d). Let $\mathcal{S}$ be the region of the (α, α_λ) plane that satisfies the conditions $\mathcal{H}' \geq 0$ and $\partial^2\mathcal{H}'/\partial\alpha^2 < 0$ (convexity condition). Consider the set of pairs $(\tilde{\alpha}, \widetilde{\alpha_\lambda})$ that are solutions of Eq. (35). Note that for a given $\widetilde{\alpha_\lambda}$, the corresponding value of $\tilde{\alpha}$ is obtained through a numerical solution of Eq. (35) (for example, using a Newton algorithm). Clearly, $\tilde{\alpha}$ maximizes $\mathcal{H}'$, provided $(\tilde{\alpha}, \widetilde{\alpha_\lambda}) \in \mathcal{S}$. Otherwise, α should be selected in order to render $\mathcal{H}' = 0$, that is, $\alpha = \pi/2$. To summarize, the optimal steering law is given by

$$\alpha = \begin{cases} \tilde{\alpha} & \text{if} \quad \mathcal{H}'(\tilde{\alpha}, \widetilde{\alpha_\lambda}) \geq 0 \\ \pi/2 & \text{if} \quad \mathcal{H}'(\tilde{\alpha}, \widetilde{\alpha_\lambda}) < 0 \end{cases} \tag{37}$$

For a 20% degradation limit, Fig. 6 shows the optimal steering law for different values of b_Σ and Σ along with the region $\mathcal{S}$ (shaded region). The boundary-value problem associated with the variational problem is consists of the equations of motion, (26) and (21), and by the Euler–Lagrange equations, (31). The boundary conditions are constrained by the planetary ephemerides. They provide 12 scalar conditions connected to the position and velocity of the solar sail at both t_0 and t_f. The other boundary condition is given by the initial value of $\Sigma(t_0) = 0$. The transversality conditions $\lambda_\Sigma(t_f) = 0$ and $\mathcal{H}(t_f) = 1$ complete the differential problem.

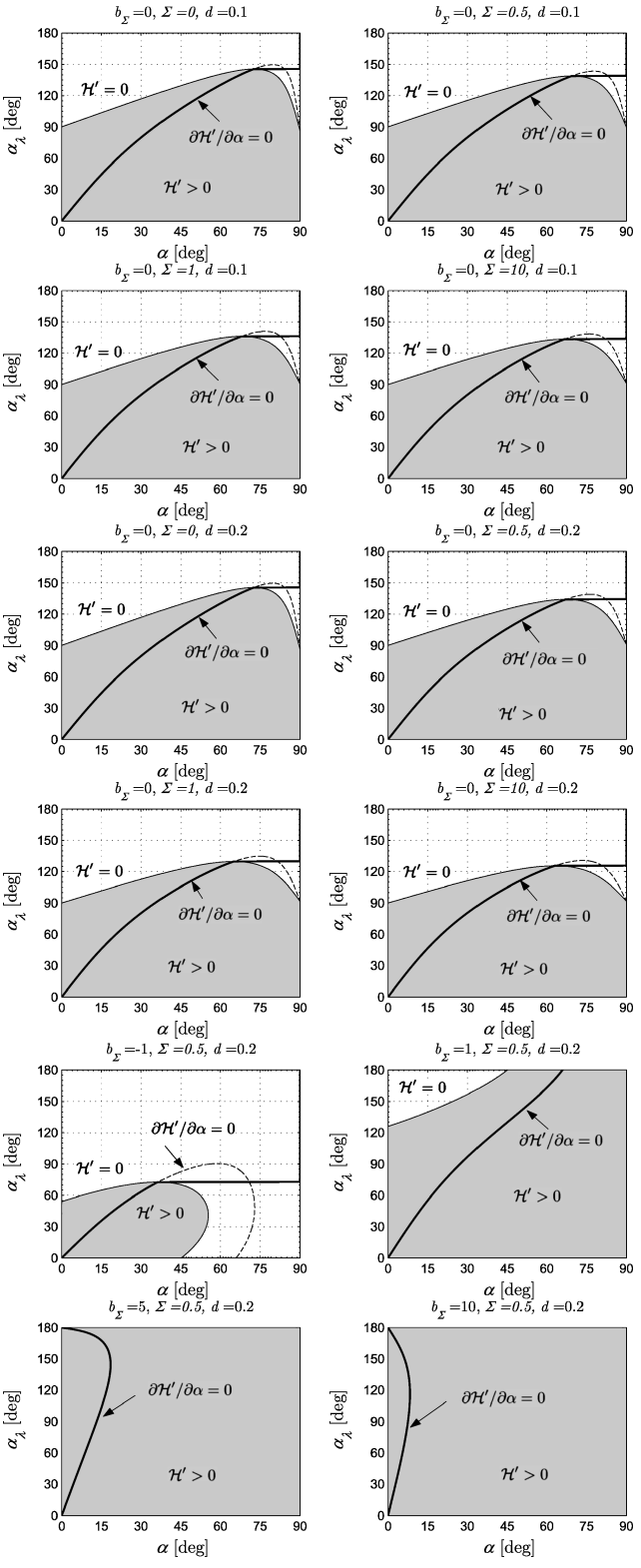

Fig. 6 Optimal control law (thick line) for the pitch angle α.

Results for Earth–Mars Orbit Transfer

To investigate the consequences of OSSD, the optimal control laws just described have been applied to a two-dimensional circular

orbit-to-orbit Earth–Mars transfer (i.e., the final position of Mars is left free) using solar sails with various lightness numbers and degradation limits. For all of the trajectories within this paper, a direct interplanetary insertion of the solar sail at Earth with zero hyperbolic excess energy ($C_3 = 0$ km^2/s^2) is assumed. The trajectories have been calculated using a hybrid numerical technique that combines genetic algorithms to obtain a rough estimate of the adjoint variables with gradient-based and direct methods to refine the solution.[12] The differential equations have been integrated in double precision using a Runge–Kutta fifth-order scheme with absolute and relative errors of 10^{-12}. A set of canonical units[17] has been used to reduce their numerical sensitivity. The impact of the OSSD model on mission performance has been investigated using three different mathematical models.

Model (a)

Within this model, an instantaneous degradation of the optical parameters of the sail is assumed. At $t = t_0$, ρ, s, and ε_f attain

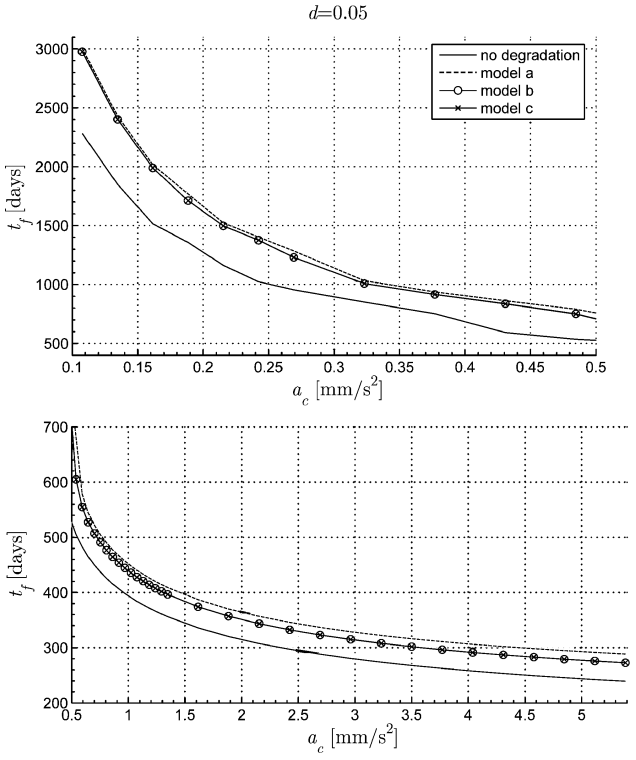

a) 5% degradation limit

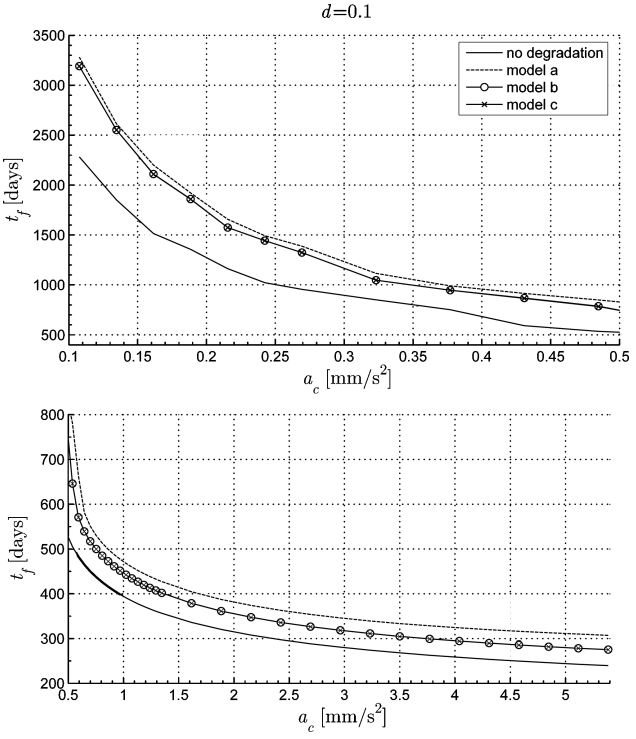

b) 10% degradation limit

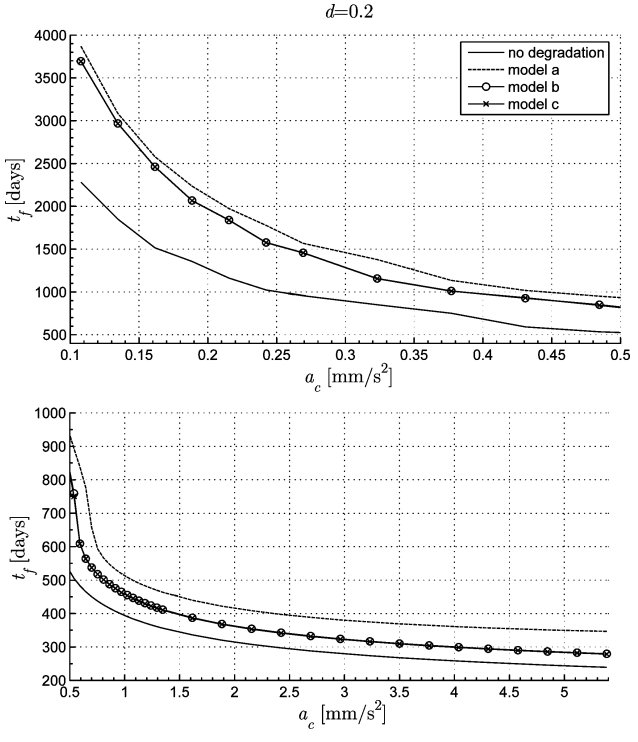

c) 20% degradation limit

Fig. 7 Trip times for a two-dimensional circular orbit-to-orbit Earth–Mars transfer using different degradation limits ($\hat{\Sigma} = 0.5$).

immediately their end-of-life values ρ_∞, s_∞, and ε_{f_∞}. From a mathematical viewpoint, this corresponds to setting $\hat{\Sigma} \to 0$, and hence $\lambda \to \infty$. Accordingly, for a given characteristic acceleration the obtained performance should be considered as an upper bound for the trip times.

Model (b)

Within this model, the degradation of the optical parameters is taken into account in the numerical integration (that is, in the equations of motion and in the Euler–Lagrange equations), but it is neglected during the evaluation of the steering law. In other words, the steering law for solar sails without degradation (given in Ref. 12) is used also for the degrading sails. From a mathematical viewpoint, this corresponds to assuming $b_\Sigma \equiv 0$ and $b_i(t) \equiv b_i(t_0)$ $(i = 1, 2, 3)$ in Eq. (35) only. This model allows one to estimate the effect of the OSSD model on the "ideal" control law (that is, on the control law obtained without taking the degradation effect into account). This simplifies the practical implementation of the steering law because the latter is a function of one time-dependent variable only (the primer vector pitch angle α_λ).

Model (c)

Within this model, the optimal control problem is solved using the OSSD model and the optimal control law described in Eq. (37).

For comparative purposes, optimal trajectories without degradation have been included in the calculations. (These correspond to the model described in Ref. 12.) Accordingly, the latter results should be considered as a lower bound for the trip times. Figure 7 summarizes the results obtained for the different models and a degradation limit of 5, 10, and 20%. Note that the trip times obtained from model (b) are nearly coincident with that from model (c) (less than 0.5% difference). The main reason for this behavior is that the values of b_Σ are small in all simulations [recall that the transversality condition requires $b_\Sigma(t_f) = 0$]. As expected, the trip times for model (a) are much greater than those obtained with noninstantaneous degradation. Finally, note that an increase of the degradation factor has remarkable consequences on trip times. This confirms that the degradation of the optical sail characteristics should not be neglected for thorough trajectory calculations and that model NPR provides excessively optimistic results.

Conclusions

Based on the current standard model for imperfectly reflecting solar sails, a new parametric model that includes the optical degradation of the sail film as a result of the erosive effects of the space environment has been presented. The primary intention of this model is not that of describing accurately the behavior of specific film-coating combinations in the real space environment, but rather that of proposing a flexible tool for representing the general optical degradation behavior of solar sails and its impact on mission analysis.

The optimal control laws for degrading solar sails have been derived using an indirect approach, and the effects of different potential degradation behaviors on trip time and sail steering have been presented for an exemplary two-dimensional circular orbit-to-orbit Earth–Mars transfer. The obtained results show that optical solar-sail degradation has a considerable effect on trip times but only a negligible effect on optimal sail steering.

Having demonstrated the potential effects of optical solar-sail degradation on future missions, an in-depth research on the real degradation behavior is now advisable. In fact, the degradation behavior of the sail's propulsive capability in a real space environment is still, to a great extent, indefinite. To narrow down the ranges of the parameters of our model, further laboratory testing has to be performed. Additionally, before a mission that relies on solar-sail propulsion is flown, the candidate solar-sail films have to be tested in the relevant space environment. Some near-term missions currently studied in the United States and in Europe would be an ideal opportunity for testing and refining the proposed degradation model.

Acknowledgments

The authors would like to thank the members of the Solar Sail Degradation Model Working Group (SSDMWG) for supporting their work: Wolfgang Seboldt (DLR, German Aerospace Center, Cologne, Germany), Colin R. McInnes (University of Strathclyde, Glasgow, Scotland), Leonel Rios-Reyes and Daniel J. Scheeres (University of Michigan, Ann Arbor, Michigan), Bong Wie (Arizona State University, Tempe, Arizona), Marianne Görlich and Franz Lura (DLR, Berlin, Germany), Benjamin Diedrich (NOAA, Silver Spring, Maryland), Volodymyr Baturkin (National Technical University of Ukraine, Kiev, Ukraine), Victoria L. Coverstone (University of Illinois at Urbana-Champaign, Urbana, Illinois), Manfred Leipold (Kayser-Threde GmbH, Munich, Germany), and Gregory P. Garbe (NASA Marshall Space Flight Center, Huntsville, Alabama).

References

[1]McInnes, C., "Delivering Fast and Capable Missions to the Outer Solar System," *Advances in Space Research*, Vol. 34, No. 1, 2004, pp. 184–191.

[2]Mengali, G., and Quarta, A. A., "Time-Optimal Three-Dimensional Trajectories for Solar Photon Thruster Spacecraft," *Journal of Spacecraft and Rockets*, Vol. 42, No. 2, 2005, pp. 379–381.

[3]Dachwald, B., "Minimum Transfer Times for Nonperfectly Reflecting Solar Sailcraft," *Journal of Spacecraft and Rockets*, Vol. 41, No. 4, 2004, pp. 693–695.

[4]Forward, R., "Grey Solar Sails," *The Journal of the Astronautical Sciences*, Vol. 38, No. 2, 1990, pp. 161–185.

[5]Wright, J. L., *Space Sailing*, Gordon and Breach, Philadelphia, 1992, pp. 227–233.

[6]McInnes, C. R., *Solar Sailing. Technology, Dynamics and Mission Applications*, Springer–Praxis Series in Space Science and Technology, Springer–Praxis, Berlin, 1999, pp. 46–53.

[7]Rios-Reyes, L., and Scheeres, D. L., "Generalized Model for Solar Sails," *Journal of Spacecraft and Rockets*, Vol. 42, No. 1, 2005, pp. 182–185.

[8]Sauer, C., "A Comparison of Solar Sail and Ion Drive Trajectories for a Halley's Comet Rendezvous Mission," AAS Paper 77-104, Sept. 1977.

[9]Cichan, T., and Melton, R. G., "Optimal Trajectories for Non-Ideal Solar Sails," AAS Paper 01-471, Aug. 2001.

[10]Dachwald, B., "Interplanetary Mission Analysis for Non-Perfectly Reflecting Solar Sailcraft Using Evolutionary Neurocontrol," *Astrodynamics 2003*, edited by J. de Lafontaine, A. Treder, M. Soyka, and J. Sims, *Advances in the Astronautical Sciences*, Vol. 116 Part 2, Univelt, Inc., San Diego, CA, 2003, pp. 1247–1262.

[11]Dachwald, B., "Optimal Solar Sail Trajectories for Missions to the Outer Solar System," *Journal of Guidance, Control, and Dynamics*, Vol. 28, No. 6, 2005, pp. 1187–1193.

[12]Mengali, G., and Quarta, A. A., "Optimal Three-Dimensional Interplanetary Rendezvous Using Nonideal Solar Sail," *Journal of Guidance, Control, and Dynamics*, Vol. 28, No. 1, 2005, pp. 173–177.

[13]Lura, F., Hagelschuer, D., Glotov, A., and Tschaly, Y., "Experiments in the Test Facility KOBE for the Investigation of Degradation Effects on Thin Foil Samples for a Solar Sail Mission Concerning the Simultaneous Influence of Space Environment Properties," 22nd Space Simulation Conference, Oct. 2002.

[14]Edwards, D., Hubbs, W., Stanaland, T., Hollerman, A., and Altstatt, R., "Characterization of Space Environmental Effects on Candidate Solar Sail Material," *Photonics for Space Environments VIII*, edited by E. Taylor, Proceedings of SPIE, Vol. 4823, The International Society for Optical Engineering, Bellingham, WA, 2002, pp. 67–74.

[15]Lawden, D., *Optimal Trajectories for Space Navigation*, Butterworths, London, 1963, pp. 54–68.

[16]Sauer, C., "Optimum Solar-Sail Interplanetary Trajectories," AIAA Paper 76-792, Aug. 1976.

[17]Seidelmann, P. K., *Explanatory Supplement to the Astronomical Almanac*, Dover Books on Mathematics, University Science Books, Sausalito, CA, 1992, pp. 696–697.